



The Effect of Al₂O₃ Coating on the Cycle Life Performance in Thin-Film LiCoO₂ Cathodes

Yong Jeong Kim,^a Tae-Joon Kim,^{a,*} Jae Wook Shin,^a Byungwoo Park,^{a,**,z}
and Jaephil Cho^{b,**}

^aSchool of Materials Science and Engineering, Seoul National University, Seoul, Korea

^bSamsung SDI Company, Limited, Kiheoung, Yongin City, Korea

The electrochemical stability of LiCoO₂ films is improved by an ~10 nm Al₂O₃ coating on top of the thin-film cathode material. Galvanostatic charge/discharge experiments showed enhanced electrochemical properties in the Al₂O₃-coated LiCoO₂ films than the bare ones. This phenomenon is related to the faster Li diffusion rate in the Al₂O₃-coated samples, as evidenced by cyclic voltammograms. This provides easier pathways for Li-ion migration by forming a thin-film solid solution layer (LiCo_{1-x}Al_xO₂). Similar results were observed in LiCoO₂ powders, showing enhanced cycle performance after coating with a thin-film metal-oxide coating. However, unlike the powder geometry, both bare and Al₂O₃-coated LiCoO₂ thin films showed negligible *c* axis expansion.

© 2002 The Electrochemical Society. [DOI: 10.1149/1.1505634] All rights reserved.

Manuscript submitted November 26, 2001; revised manuscript received April 2, 2002. Available electronically August 21, 2002.

Thin-film microbatteries¹⁻³ have potential applications in micro-electronics. In particular, the fabrication of lithiated intercalation oxides in a thin-film form is of great interest because of their possible use as a positive electrode in all-solid-state lithium rechargeable microbatteries. Crystalline LiCoO₂ films have been most widely investigated as cathode material in rechargeable microbatteries due to their high energy density and relatively good cycle life performance.⁴⁻¹² This cathode has a hexagonal α -NaFeO₂ structure with alternating planes containing Li and Co ions separated by close packed oxygen layers. However, this material shows relatively great capacity fading after extended cycling when Li ions become deintercalated above 4.2 V. This was reported to be due to anisotropic expansion and contraction during cycling.¹³⁻¹⁸

In an attempt to overcome this problem in the powder geometry, Cho *et al.*¹⁶⁻¹⁸ reported that thin film metal-oxide coating (Al₂O₃, ZrO₂, etc.) on the powder surface improved the capacity retention of LiCoO₂ cathodes. These metal-oxide coated powders exhibited no deterioration in their initial capacities, and also excellent capacity retention above 4.2 V relative to the uncoated cathodes. This phenomenon was attributed to a suppression of expansion of the lattice constant *c*.¹⁶⁻¹⁸ In this paper, a novel coating technology for improving the cycle life performance in LiCoO₂ thin-film cathodes is reported.

Experimental

LiCoO₂ thin-film deposition.—LiCoO₂ films were deposited by radio frequency (rf) magnetron sputtering using a LiCoO₂ target on top of the ~200 nm thick Pt current collector on SiO₂ (~150 nm)/Si substrate. To improve Pt adhesion to the substrate, an ~10 nm thick TiO₂ underlayer was deposited by reactive sputtering of a Ti target. The LiCoO₂ target was prepared by cold pressing and sintering LiCoO₂ powders at 1000°C for 10 h in air. A binder was added to the powders to aid sintering, and the targets were bonded to copper backing plates with indium to the magnetron gun. The targets were sputtered at a working pressure of 20 mTorr with Ar/O₂ = 3/1. An rf power of 100 W was applied to the target, and the average deposition rate was 1.8 nm/min. To crystallize the as-deposited amorphous films, *ex situ* annealing treatment of all rf-sputtered films was performed in flowing O₂ at 700°C for 2 h.

After crystallization, an ~10 nm thick Al₂O₃ thin film was deposited on top of the LiCoO₂ thin films, by reactive sputtering of an

Al target. In order to form an LiCo_{1-x}Al_xO₂ solid solution near the LiCoO₂ film surface, the coated samples were annealed at 400°C for 10 h in an O₂ atmosphere.¹⁶⁻¹⁸ The structural characterizations of these films were carried out by *ex situ* X-ray diffraction (XRD) and scanning electron microscopy (SEM). To characterize the concentration profile near the Al₂O₃-coated LiCoO₂ film surface, Auger electron spectroscopy (AES) was performed.

Electrochemical analysis.—The electrochemical behaviors of Al₂O₃-coated LiCoO₂ films were investigated by both galvanostatic charge/discharge experiments and cyclic voltammetry. Beaker-type half cells were used to evaluate the electrochemical properties of both uncoated and Al₂O₃-coated LiCoO₂ films. The electrochemical cells consisted of Li-metal sheets as a counter and reference electrode, a cathode film of an 1 cm² active area as a working electrode, and 1 M LiPF₆ in ethyl carbonate/dimethyl carbonate (EC/DEC, 1/1 vol % Cheil Industries, Inc.) as a liquid electrolyte. Typically, the as-fabricated cells had an open-circuit voltage (OCV) of approximately 2.7 V, but values between 1.8 and 2.9 V were also observed. These cells were cycled

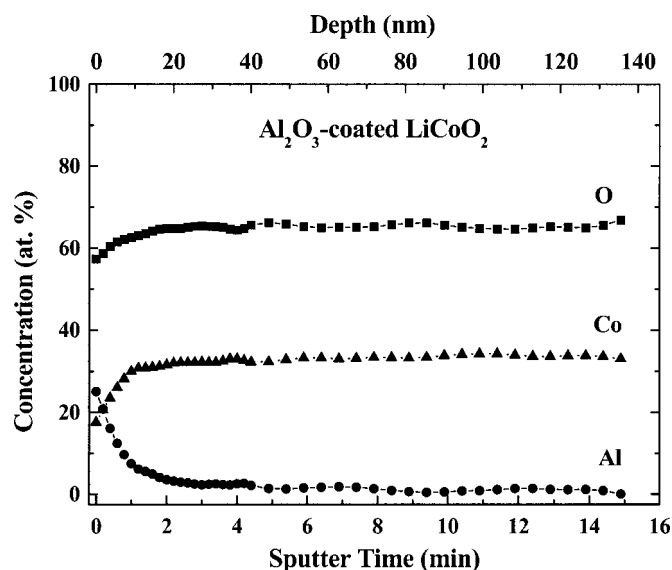


Figure 1. Concentration/depth profile of an Al₂O₃-coated LiCoO₂ thin-film cathode.

* Electrochemical Society Student member.

** Electrochemical Society Active Member.

^z E-mail: byungwoo@snu.ac.kr

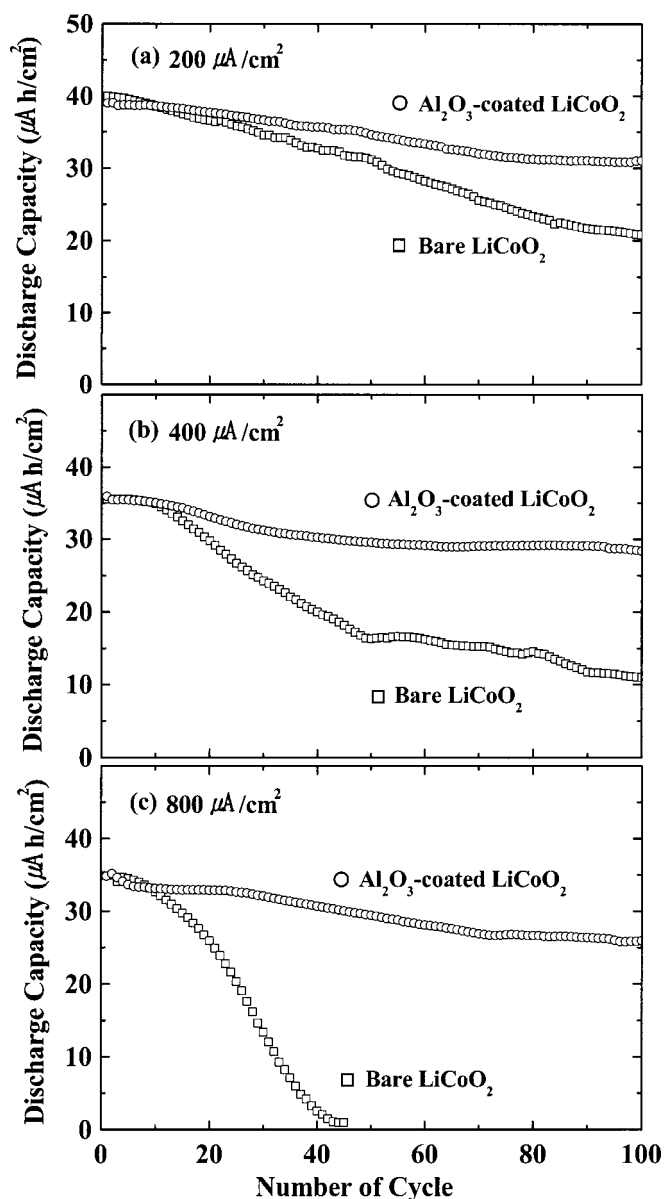


Figure 2. Cycle life performance (discharge capacity vs. cycle number) of uncoated and Al_2O_3 -coated LiCoO_2 thin films between 4.4 and 2.75 V up to 100 cycles. The current rates are (a) $200 \mu\text{A}/\text{cm}^2$, (b) $400 \mu\text{A}/\text{cm}^2$, and (c) $800 \mu\text{A}/\text{cm}^2$.

between 4.4 and 2.75 V for up to 100 cycles at current rates ranging from 100 to $800 \mu\text{A}/\text{cm}^2$. At all the charge/discharge cutoff steps, the voltages were potentiostated until the current decreased to 10% of the charge/discharge rates.

Results and Discussion

The thickness of the thin-film LiCoO_2 cathode determined by profilometry and direct observation of the fractured cathode through field emission (FE)SEM was approximately 550 nm. The grain size obtained in plan-view SEM was approximately 250 nm. AES analysis of the Al_2O_3 -coated LiCoO_2 thin film was carried out to examine the distribution of Al atoms near the film surface (Fig. 1). The results show that a significant amount of Al atoms are distributed at the surface, and Al atoms are distributed within ~ 10 nm of the film surface with a decreasing concentration gradient, indicating the formation of a thin-film solid solution ($\text{LiCo}_{1-x}\text{Al}_x\text{O}_2$). The sputter rate was estimated to be 9.1 nm/min, as calibrated from SiO_2 . Be-

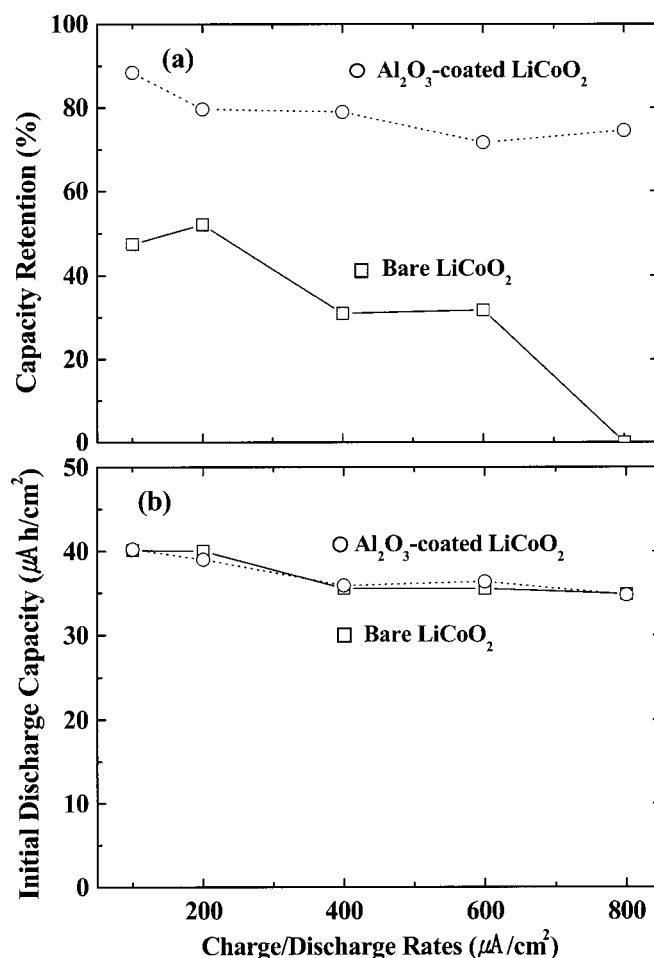


Figure 3. (a) Capacity retention vs. current rates after 100 cycles, and (b) initial capacity vs. current rates of uncoated and Al_2O_3 -coated LiCoO_2 films.

cause the error range from the Li composition is relatively large in the Auger measurements due to its low atomic number, its composition is excluded in Fig. 1.

In order to test the cycle-life performance of bare and Al_2O_3 -coated LiCoO_2 thin films, two electrode-half cells were cycled at various current rates between 4.4 and 2.75 V. Until recently, in the thin-film LiCoO_2 cathodes, few researchers have deintercalated Li ions up to 4.4 V because of their rapid capacity fading.^{5-7,10,11} The Al_2O_3 -surface coating significantly enhanced the capacity retention of the LiCoO_2 thin-film cathodes. As shown in Fig. 2, the discharge capacity of Al_2O_3 -coated LiCoO_2 after 100 cycles was $\sim 80\%$ of the original capacity, while that of bare LiCoO_2 deteriorated to $\sim 52\%$ of the initial capacity at the current rate of $200 \mu\text{A}/\text{cm}^2$. In particular, the Al_2O_3 -coated samples show excellent capacity retention ($\sim 75\%$) even at $800 \mu\text{A}/\text{cm}^2$ over 100 cycles. In contrast, bare LiCoO_2 sample retained $\sim 3\%$ of its original capacity after only 45 cycles (Fig. 2c). The effect of the Al_2O_3 coating on the cycle life performance was more pronounced at a high-current rate. Capacity retention of both the bare and Al_2O_3 -coated thin films as a function of the current rate is shown in Fig. 3a. The rate of capacity fading was reduced largely by the ~ 10 nm Al_2O_3 surface coating. In addition, the initial discharge capacities of the Al_2O_3 -coated LiCoO_2 films were close to those of the uncoated ones (Fig. 3b). The enhanced rate capability in Al_2O_3 -coated films results from easier pathways for Li-ion diffusion through the coated layer. However, the detailed mechanisms including potential corrosive reaction at the surface need to be identified.

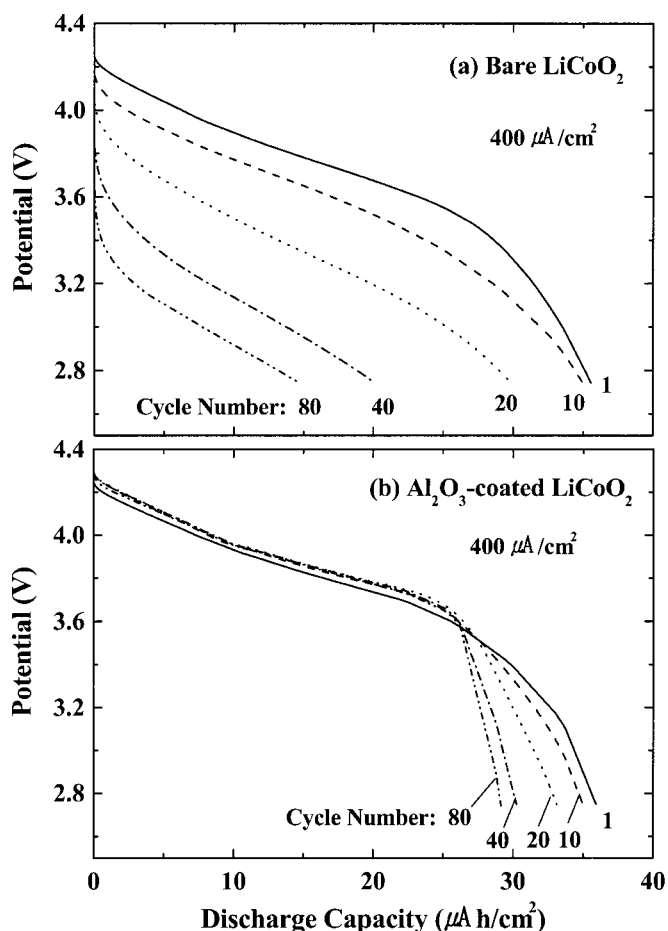


Figure 4. Voltage profiles of (a) uncoated and (b) Al_2O_3 -coated LiCoO_2 films between 4.4 and 2.75 V at the rate of $400 \mu\text{A}/\text{cm}^2$.

Figure 4 shows that the voltage profiles of the coated LiCoO_2 thin films are higher than those of the bare films with the cycling number increasing to 80 cycles at $400 \mu\text{A}/\text{cm}^2$. This is related to the faster Li-ion diffusivities in the coated samples, as evidenced by the cyclic voltammogram (CV) data (Fig. 5). The formation of the solid solution ($\text{LiCo}_{1-x}\text{Al}_x\text{O}_2$) near the LiCoO_2 surface through the Al_2O_3 coating causes easier diffusion paths. The enhanced Li diffusion in Al-doped LiCoO_2 powder has been reported.¹⁹ To investigate any possibility of surface (corrosion) reaction with the liquid electrolyte (such as Co dissolution), inductively coupled plasma-mass spectroscopy analysis of the electrolyte is performed after 100 cycles. However, the amount of Co dissolution in liquid electrolyte (with 10 mL) is ~ 0.2 ppm for both bare and Al_2O_3 -coated thin films, showing that the Co dissolution from $\text{Li}_{1-x}\text{CoO}_2$ cathode is below the level of detectability.

The kinetics of Li-ion diffusion in the LiCoO_2 films are important factors in the battery operation since they govern the intercalation/deintercalation rates. To investigate both the phase transformations and the kinetics of Li-ion diffusion, the CVs of both bare and Al_2O_3 -coated samples were carried out up to the sixth cycle (Fig. 5). The widths of both the anodic and cathodic peaks are sharpened by the Al_2O_3 surface coating, as shown in Fig. 5 and 6. In addition, as the cycle number increases, the Al_2O_3 -coated LiCoO_2 films have a smaller peak separation between the anodic and cathodic peak, compared to the bare samples. These results suggest that the diffusion and migration of Li ions are faster in the Al_2O_3 -coated LiCoO_2 films than in the bare films. Figure 6 represents changes in the peak widths and peak separation as a function

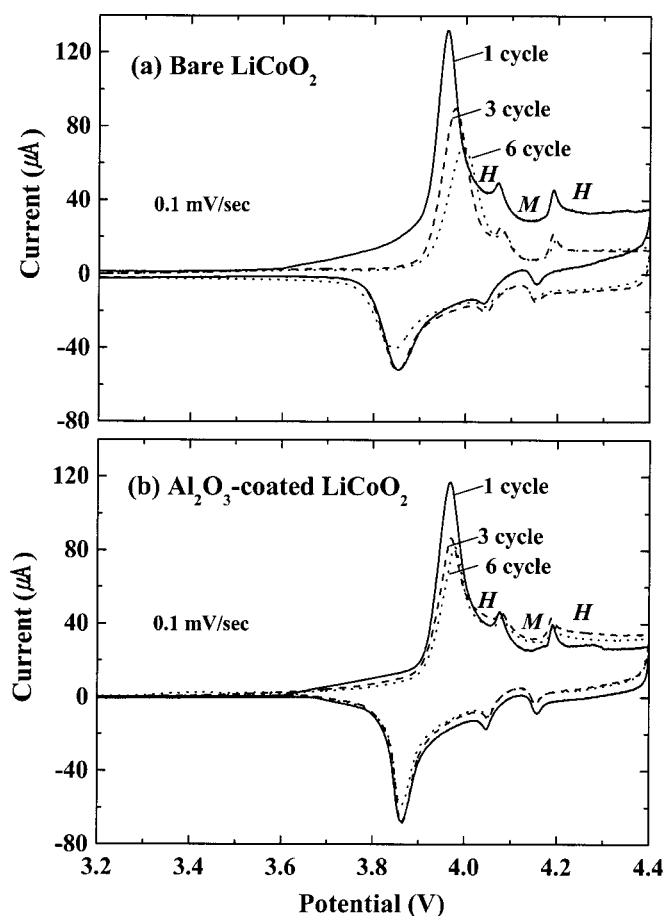


Figure 5. Cyclic voltammograms of (a) uncoated and (b) Al_2O_3 -coated LiCoO_2 films. The sweep rate was $0.1 \text{ mV}/\text{s}$, and the symbols *H* and *M* indicate the hexagonal and monoclinic phases, respectively.

of the cycle number, as obtained from fitting the anodic and cathodic peaks (Fig. 5) corresponding to the two-phase hexagonal region at ~ 3.96 and ~ 3.86 V, respectively, with a Lorentzian function. Moreover, it is intriguing that the cathodic peak of the uncoated sample is wider than the Al_2O_3 -coated sample, while the enhancement in the anodic peak is not that significant.

As shown in Fig. 5, Al_2O_3 -coated LiCoO_2 thin films have a monoclinic phase, at ~ 4.15 V from deintercalation (charging) and at ~ 4.10 V from intercalation (discharging). In contrast, the Al_2O_3 coating (~ 10 nm) on the LiCoO_2 powders ($\sim 10 \mu\text{m}$) showed enhanced capacity retention, by the disappearance of the phase transition from the hexagonal to monoclinic phase.^{14,15} The LiCoO_2 thin films are strongly textured along the (003) plane, as shown in Fig. 7a. Because the *c* axis expansion perpendicular to the (003) plane may not be suppressed effectively by the Al_2O_3 coating parallel to the (003) plane, the phase transition from the hexagonal to monoclinic phase may occur as shown in Fig. 5b. However, the lattice constants as a function of the cell voltage in $\text{Li}_{1-x}\text{CoO}_2$ from the OCV to 4.40 V show negligible *c* axis expansion in both the bare and Al_2O_3 -coated $\text{Li}_{1-x}\text{CoO}_2$ thin films (Fig. 8), whereas the uncoated $\text{Li}_{1-x}\text{CoO}_2$ powders exhibited $\sim 2.6\%$ *c* axis expansion at $x \approx 0.5$ (4.2 V).¹⁸ The cycle life performance in the various metal-oxide-coated LiCoO_2 powders correlated with the suppression of *c* axis expansion.¹⁸ However, in the ~ 550 nm thin-film LiCoO_2 cathodes, distinguishing the small lattice constant expansion from the bare and the Al_2O_3 -coated LiCoO_2 films is difficult with the current experimental XRD resolution.

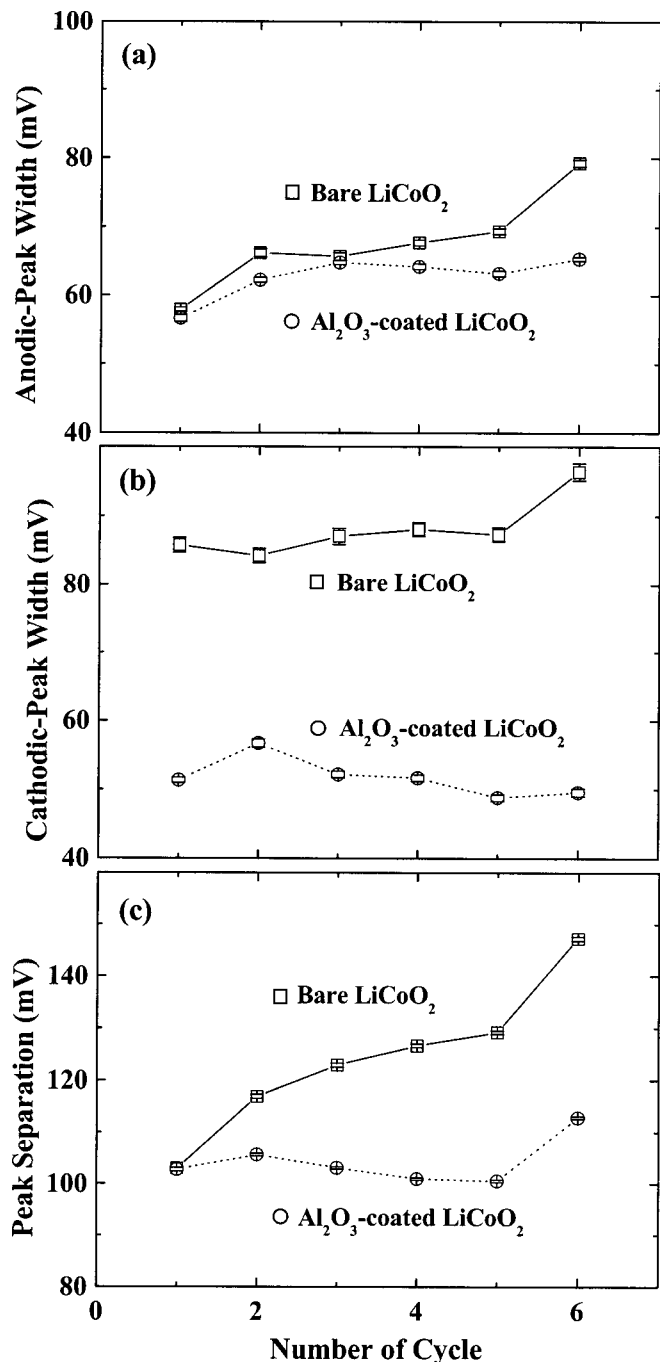


Figure 6. Changes in the (a) anodic peak width, (b) cathodic peak width, and (c) peak separation between the anodic and cathodic peak, from the uncoated and Al₂O₃-coated LiCoO₂ samples up to the 6th cycle.

The XRD patterns in Fig. 7a show that the Al₂O₃-coated LiCoO₂ thin films (heat-treated at 400°C) exhibit a strong (003) texture of hexagonal LiCoO₂, similar to the case of the bare LiCoO₂ thin films. Those XRD patterns show no peaks of any Al₂O₃ phase, suggesting that the ~10 nm Al₂O₃ coating layer exists as either an amorphous phase or as a solid solution (LiCo_{1-x}Al_xO₂) by interdiffusion, as indicated by AES. To investigate the structural modification after cycling for both the uncoated and Al₂O₃-coated LiCoO₂, three peaks of (003), (006), and (009) were fitted from Fig. 7a and b, respectively, before and after cycling. Peaks of the uncoated LiCoO₂ are broadened after 100 cycles, whereas those of the Al₂O₃-coated LiCoO₂ thin films do not show any noticeable peak broadening (Fig.

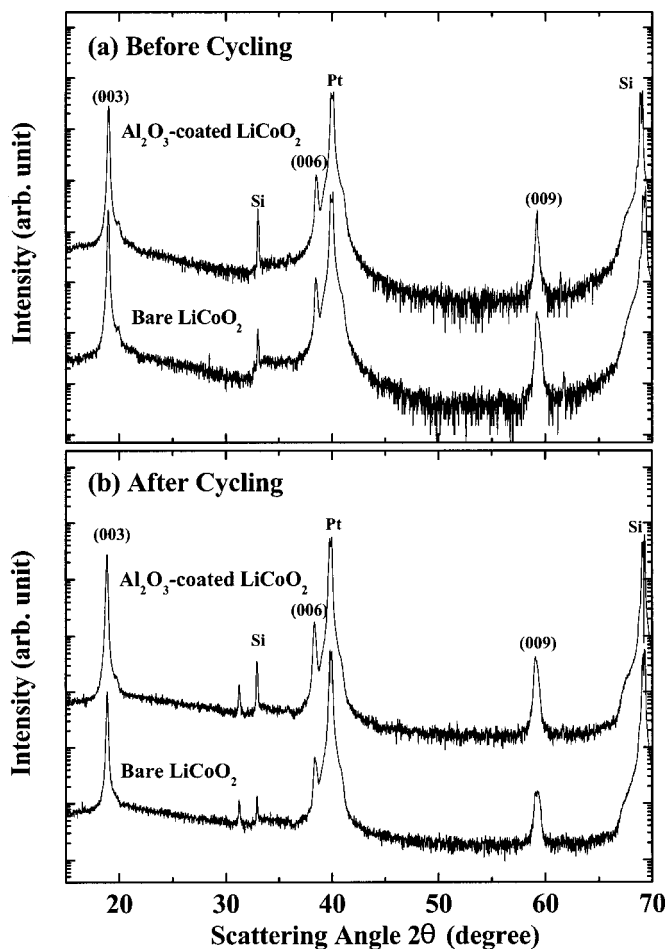


Figure 7. XRD patterns of uncoated and Al₂O₃-coated LiCoO₂ films (a) before cycling, and (b) after 100 cycles. After 100 cycles, each cell was potentiostated for 1 h at 2.75 V. The peak at $2\theta = 31.3^\circ$ after cycling is due to the formation of Co₃O₄.

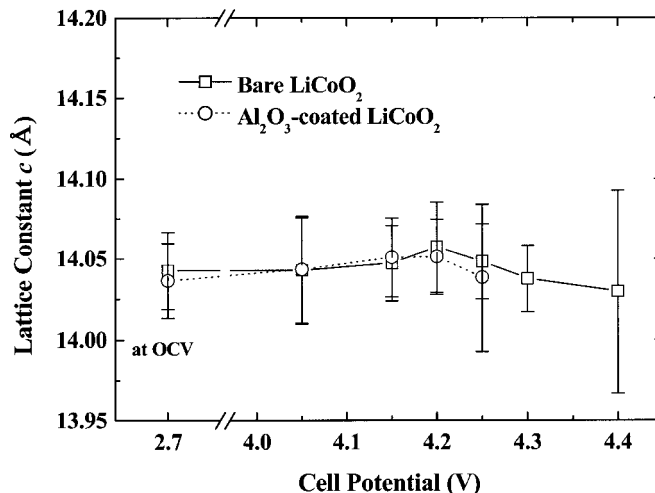


Figure 8. Changes in the lattice constant c as a function of the cell potential for uncoated and Al₂O₃-coated LiCoO₂ films. Each cell was charged at 100 $\mu\text{A}/\text{cm}^2$ rate to the predetermined voltages, then potentiostated until the current decreased to 1 $\mu\text{A}/\text{cm}^2$.

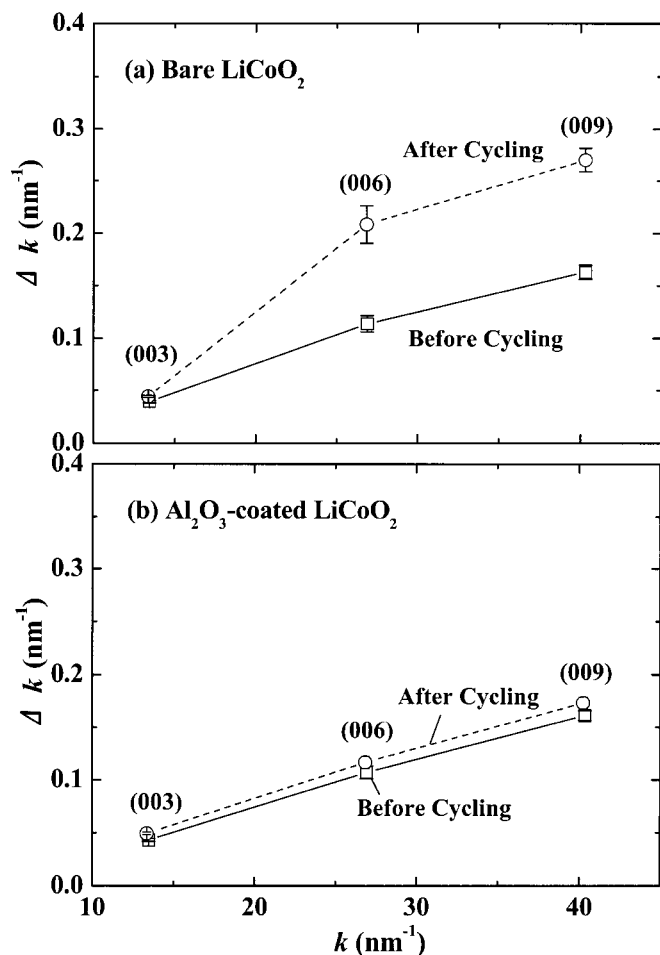


Figure 9. Plots of Δk vs. k in the (a) uncoated and (b) Al₂O₃-coated LiCoO₂ films, before cycling and after 100 cycles. After 100 cycles, each cell was potentiostated for 1 h at 2.75 V.

9). Such peak broadening may be associated with the microstructural defects or local strain.²⁰ The XRD peak widths Δk (full width at half-maximum) were fitted for each peak with the scattering vector $\mathbf{k} = (4\pi/\lambda)\sin \theta$, using a double-peak Lorentzian function.²⁰ To eliminate the instrumental broadening effect in diffraction, a resolution function ($\Delta k_{\text{resol}} = 0.046 + 0.0004 k \text{ nm}^{-1}$ for $K\alpha_1$) estimated from silicon was subtracted after fitting each diffraction peak. As shown in Fig. 9a for bare LiCoO₂ thin films, the slope of Δk vs. k representing the local strain ($\Delta d/d$) increases from $0.48 \pm 0.04\%$ before cycling to $0.87 \pm 0.11\%$ after cycling. In contrast, the Al₂O₃-coated LiCoO₂ samples shows negligible change in the slope of Δk vs. k after 100 cycles (before cycling: $0.44 \pm 0.01\%$, and after cycling: $0.47 \pm 0.02\%$), indicating that the local strain did

not further develop after cycling. Further studies are currently under way to detail the mechanisms responsible for the Al₂O₃ surface coating suppressing the XRD peak broadening during electrochemical cycling, by performing cross-sectional transmission electron microscopy.

Conclusions

The cycle life performance of LiCoO₂ thin films was improved by an ~ 10 nm Al₂O₃ coating. Even though the Al₂O₃-coated LiCoO₂ films had a phase transition to a monoclinic phase at 4.15 V (during charging), unlike the Al₂O₃-coated powders, the capacity retention in the thin-film geometry was significantly enhanced by the Al₂O₃ coating, especially at high-current rates. These results correlate with the enhanced diffusivity of Li ions in the Al₂O₃-coated LiCoO₂ thin films (from CVs). In addition, the Al₂O₃ coating prevents any local strain development during cycling, as confirmed by the Δk vs. k slope.

Acknowledgments

This work is supported by Korea Institute of Industrial Technology Evaluation and Planning, in Ministry of Commerce, Industry and Energy.

One of the authors, B. Park, assisted in meeting the publication costs of this article.

References

1. P. Birke, W. F. Chu, and W. Weppner, *Solid State Ionics*, **93**, 1 (1997).
2. J. B. Bates, G. R. Gruzalski, N. J. Dudney, C. F. Luck, and X. Yu, *Solid State Ionics*, **70-71**, 619 (1994).
3. C. Julien and G.-A. Nazri, *Solid State Batteries: Materials Design and Optimization*, Kluwer Academic Publishers, Boston (1994).
4. P. J. Bouwman, B. A. Boukamp, H. J. M. Bouwmeester, H. J. Wondergem, and P. H. L. Notten, *J. Electrochem. Soc.*, **148**, A311 (2001).
5. J. B. Bates, N. J. Dudney, B. J. Neudecker, F. X. Hart, H. P. Jun, and S. A. Hackney, *J. Electrochem. Soc.*, **147**, 59 (2000).
6. B. Wang, J. B. Bates, F. X. Hart, B. C. Sales, R. A. Zuhr, and J. D. Robertson, *J. Electrochem. Soc.*, **143**, 3203 (1996).
7. J.-K. Lee, S.-J. Lee, H.-K. Baik, H.-Y. Lee, S.-W. Jang, and S.-M. Lee, *Electrochem. Solid-State Lett.*, **2**, 512 (1999).
8. M. U. Kleinke, J. Davalos, C. Polo da Fonseca, and A. Gorenstein, *Appl. Phys. Lett.*, **74**, 1683 (1999).
9. F. X. Hart and J. B. Bates, *J. Appl. Phys.*, **83**, 7560 (1998).
10. K. A. Striebel, C. Z. Deng, S. J. Wen, and E. J. Cairns, *J. Electrochem. Soc.*, **143**, 1821 (1996).
11. J. D. Perkins, C. S. Bahn, J. M. McGraw, P. A. Parilla, and D. S. Ginley, *J. Electrochem. Soc.*, **148**, A1302 (2001).
12. Y.-I. Jang, B. J. Neudecker, and N. J. Dudney, *Electrochem. Solid-State Lett.*, **4**, A74 (2001).
13. H. Wang, Y.-I. Jang, B. Huang, D. R. Sadoway, and Y.-M. Chiang, *J. Electrochem. Soc.*, **146**, 473 (1999).
14. T. Ohzuku and A. Ueda, *J. Electrochem. Soc.*, **141**, 2972 (1994).
15. J. N. Reimers and J. R. Dahn, *J. Electrochem. Soc.*, **139**, 2091 (1992).
16. J. Cho, Y. J. Kim, and B. Park, *Chem. Mater.*, **12**, 3788 (2000).
17. J. Cho, Y. J. Kim, and B. Park, *J. Electrochem. Soc.*, **148**, A1110 (2001).
18. J. Cho, Y. J. Kim, T.-J. Kim, and B. Park, *Angew. Chem. Int. Ed. Engl.*, **40**, 3367 (2001).
19. S.-T. Myung, N. Kumagai, S. Komaba, and H.-T. Chung, *Solid State Ionics*, **139**, 47 (2001); J. D. Perkins, C. S. Bahn, J. M. McGraw, P. A. Parilla, and D. S. Ginley, *J. Electrochem. Soc.*, **148**, A1302 (2001).
20. Y. Kim, J. Oh, T.-G. Kim, and B. Park, *Appl. Phys. Lett.*, **78**, 2363 (2001).